A perceptually inspired Driver Model for Speed Control in curves

Gruppelaar, Virgilio; van Paassen, Rene; Mulder, Max; Abbink, David

DOI
10.1109/SMC.2018.00220

Publication date
2018

Document Version
Accepted author manuscript

Published in
Proceedings 2018 IEEE International Conference on Systems, Man, and Cybernetics

A perceptually inspired Driver Model for Speed Control in curves

Virgílio Gruppelaar, M. M. (René) van Paassen, Max Mulder
Faculty of Aerospace Engineering, TU Delft
Delft, the Netherlands 2629 HS
Email: {M.M.vanPaassen; M.Mulder}@tudelft.nl
David A. Abbink
Faculty of Mechanical, Materials and Maritime Engineering, TU Delft
Delft, the Netherlands 2629 HS
Email: D.A.Abbink@tudelft.nl

***Abstract*—Understanding speed control in driving is important for analysis of road geometry and for the development of driver support assistance devices. Current models for speed selection are primarily based on the relation between road geometry and observed speeds. This study proposes a more detailed model that relates individual speed control to accelerator and brake pedal, based on perception of the visual scene as captured by the Extended Tangent Point (ETP). We investigated the potential of the the Time to ETP (TETP) as input for accelerator and brake pedal control. Based on observations from driving studies, we propose a model, and tuning rules to adjust the model parameters to observed behavior. A simulator experiment showed that, after individualization of the thresholds using a binary classification method, the model is capable of accurately capturing individual speed adaptation of 15 drivers on single lane roads with multiple curves.**

I. Introduction

When driving on a curved road, people need to adjust their speed to the road shape. Field studies show a correlation between curve radius and speed [1]–[3]. Other geometrical factors that can influence speed choice are the road width [4], the lengths of the straight road sections between curves, the curve deflection angle, the presence of other curves in close proximity, and the curve superelevation [5]. In addition to this, the lateral position of the vehicle on the road can alter the effective turn radius, impacting drivers' speed choice [6].

In the context of road design and road safety, many studies model the speed at which a driver can safely negotiate a turn based on the geometrical characteristics of that turn. While this is a useful limit for assistance systems to take into account as an upper boundary, it does not provide information about a driver's desired speed and is consequently not directly usable in Advanced Driver Assistance Systems (ADAS) applications [7]. We wish to model the manner in which drivers themselves choose their speed, depending on their preference of driving style, risk, or safety margins.

The majority of models for speed adaptation when approaching a curve propose a relationship between road curvature and speed, fitting parameters to experimental data [1], [2], [7], [8]. In order to account for the effects of the geometry of the turn, adjacent road segments, and lateral position, model complexity will increase [5], [6], [9]. An issue with these models is that human drivers have been shown to be rather poor judges of road curvature [10], which suggests that other cues must play a role.

During driving, humans tend to control their risk by employing certain safety margins [11]. In situations where speed needs to be adjusted, these are usually time margins such as the Time to Line Crossing (TLC) in lane keeping [12] or the Time Headway and Time To Contact in car following [13]. Contrasting with their poor performance in judging distances, velocities, and curvatures [10], humans can very accurately judge visual angles and time margins to target or contact points [14]. This leads us to believe that speed adjustment in turns is very likely dependent on a time margin to a salient point.

Land and Lee [15] introduced the idea that the Tangent Point (TP) on the inside of a curve is key to curve negotiation, and a substantial amount of research has shown that drivers focus their gaze towards the area containing the apex of the curve, employing what is called TP orientation [16]. However, driver eye movement studies have shown that drivers do not fixate only on this point, but also scan areas farther up the road in a controlled pattern [17]. A particular area of interest is the *far road triangle* [18], comprised of the TP, the Occlusion Point (OP), which is the farthest point of the road that is not blocked by obstacles in the field of vision, and the point where the driver's line of vision through the TP intersects the opposite lane edge, the Extended Tangent Point (ETP).

In this paper we present a novel model for driver speed choice based on ETP perception. The model additionally relates this speed choice to driver's longitudinal control inputs (depression of brake pedal and gas pedal), based on threshold values. Section II describes the approach taken in designing the model, the developed speed control algorithm, and predictions from simulations. To validate the model an experiment was set up and performed, as shown in Section III. The results from this experiment are shown and discussed in Sections IV and V.

II. Model design

Our model for speed choice is based on the Time to Extended Tangent Point (TETP), which is defined as the time

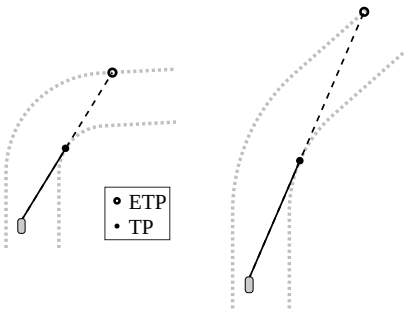

Fig. 1. Location of Tangent Point (TP) and Extended Tangent Point (ETP) for two curves with different radii and deflection angles.

it would take for the vehicle to reach the ETP in a straight line, if speed would not be changed. This time margin can be interpreted as a measure of how much the road 'opens up' after a turn, see Figure 1. As can be imagined, the TETP will also depend on the lateral position of the vehicle with respect to the road, making it a parameter sensitive to the driven trajectory, rather than merely depending on the road geometry.

To investigate the viability of this model approach, we calculated TETP for data obtained from an earlier experiment performed at the Human-Machine Interaction (HMI) Laboratory of TU Delft [19], which studied driver's speed choice for curved roads. Our preliminary analysis illustrated that speed decrease before a curve occurred first in a 'deceleration zone', potentially following by a 'braking zone', each correlated with two different time margins. Drivers first released the accelerator when the TETP decreased beyond a certain threshold value (deceleration zone), and would only begin to press the brake pedal when the TETP exceeded a second, lower threshold (the braking zone). Observations of mid-corner and corner exit behavior also showed a correlation between acceleration behaviour and TETP. More spefically, close to the end of the decelerating or braking zones, the TETP decreased more slowly, eventually becoming constant, before increasing again as a consequence of the road opening up after the turn. Drivers appeared not to use the same time thresholds for accelerating as for decelerating, but became comfortable once the rate of change of the TETP approached zero. Then, drivers began accelerating, and only if the TETP started decreasing again did they resume decelerating or braking.

The analysis also illustrated that, as could be expected, each driver behaves differently. Some drivers never adapted their speed to the given road, while others felt the need to brake in certain curves. This can be attributed to the idea that different drivers feel comfortable at different TETP values. By identifying these different thresholds, and combining them with different gains on gas and brake pedal deflection, it could be possible to use a TETP-based approach to model each driver's individual preferences in speed choice and the associated longitudinal control actions.

These findings led us to develop our model of driver speed control through pedal actuation, based on TETP thresholds as the primary perceptual variables.

A. Model architecture

The speed control model distinguishes five phases of speed control during cornering: *acceleration*, *deceleration*, *braking*, *brake release*, and *re-acceleration*. Which of the five phases of the model is active, is determined by three time thresholds parameters: a TETP threshold for deceleration (releasing the gas pedal) and a lower one for braking, and a threshold on the TETP rate of change.

The model regulates vehicle speed using these three time threshold parameters, along with three associated actuation gains to describe the magnitude of the corresponding pedal actuations in each phase. The six parameters are:

- T_d [s]: The minimum TETP before a driver releases the accelerator pedal to enter the *deceleration* phase.
- K_d [-]: The accelerator pedal release gain, determining how quickly the driver lets go of the gas pedal during the *deceleration* phase.
- T_b [s]: The minimum TETP before a driver presses the brake pedal to enter the *braking* phase.
- K_b [-]: The brake pedal depression gain, determining how strongly the driver presses the brake pedal during the *braking* phase.
- $\mathrm{d}T_a$ [-]: The rate of change of TETP at which the driver feels comfortable to begin accelerating out of a curve. It determines when the *brake release* and *re-acceleration* phases begin, if the model is already in the *braking* or *deceleration* phases, respectively.
- K_a [-]: The accelerator pedal depression gain. This parameter eterminines how strongly the driver presses the accelerator pedal during the *acceleration*, *brake release* and *re-acceleration* phases.

A typical example of how the model works is shown in Figure 2, where a simulated vehicle negotiates a 150m radius left turn with a target speed of 27ms^{-1} on the straight sections. In this figure, we can clearly see the differences between the phases of the model.

B. Speed control algorithm

The algorithm the model uses to select one of the five phases, based on the three thresholds T_d, T_b and $\mathrm{d}T_a$, is illustrated in Figure 3. The calculations for the different phases are described below:

1) *Acceleration*: If the current TETP is above the deceleration threshold T_d, the model will go into the *acceleration* phase, where the brake pedal deflection is $\delta_b = 0$ and the accelerator pedal deflection, δ_a, is limited only by the maximum speed on the road segment, as described by:

$$\delta_a = \delta_{a,EB} + K_a \left(1 - \frac{V}{V_{max}}\right) \tag{1}$$

2) *Deceleration*: If the TETP is below the deceleration limit T_d, but above the braking limit T_b, the model is in the *deceleration* phase. In this case, the brake pedal deflection continues to be zero, while the desired accelerator pedal deflection is a function of how far the TETP is from both

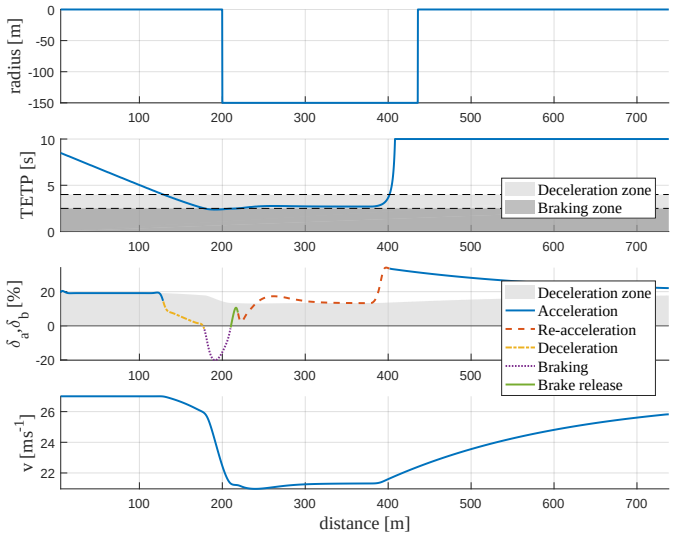

Fig. 2. Driver model simulation of speed control for a 150m radius left turn (negative radius in the top panel), showing TETP, pedal deflections, and speed. In the third panel, positive pedal deflections correspond to the accelerator pedal, while negative deflections represent brake actuation. The five phases are shown with different line styles, and the shaded area represents the deceleration zone: accelerator pedal position values that correspond to a zero or negative acceleration.

thresholds, as described by Equation (2). The resulting value is bound between the accelerator pedal deflection required to maintain the current speed, $\delta_{a,EB}$, and 0.

$$\delta_a = \min\left(\delta_{a,EB}, K_d\left(\frac{\text{TETP} - T_b}{T_d - T_b}\right)\right) \tag{2}$$

This phase will continue until either the TETP goes under the braking threshold T_b and the *braking* phase starts, or the (filtered) rate of change of the TETP approaches zero, at which point the *re-acceleration* phase begins.

3) *Braking*: If the TETP is below the braking threshold, the accelerator pedal deflection is set to zero, while the brake pedal deflection is dependent on the ratio between the current TETP and T_b, as described in:

$$\delta_b = K_b\left(1 - \frac{\text{TETP}}{T_b}\right) \tag{3}$$

4) *Brake release*: As the vehicle brakes, the TETP will gradually stop decreasing. If the rate of change of TETP becomes larger than $\mathrm{d}T_a$ while the braking phase is active, the *brake release* phase begins. The brake pedal deflection is the same as in the *braking* phase (Equation (3)), with the added limitation that the deflection cannot increase while this phase is active. While the vehicle is braking, there should be no accelerator pedal actuation ($\delta_a = 0$). During this phase, once δ_b becomes 0, the model will begin pressing the accelerator pedal. The deflection δ_a is then the minimum value between the pedal position from the acceleration phase, and a direct function of the rate of change of the TETP:

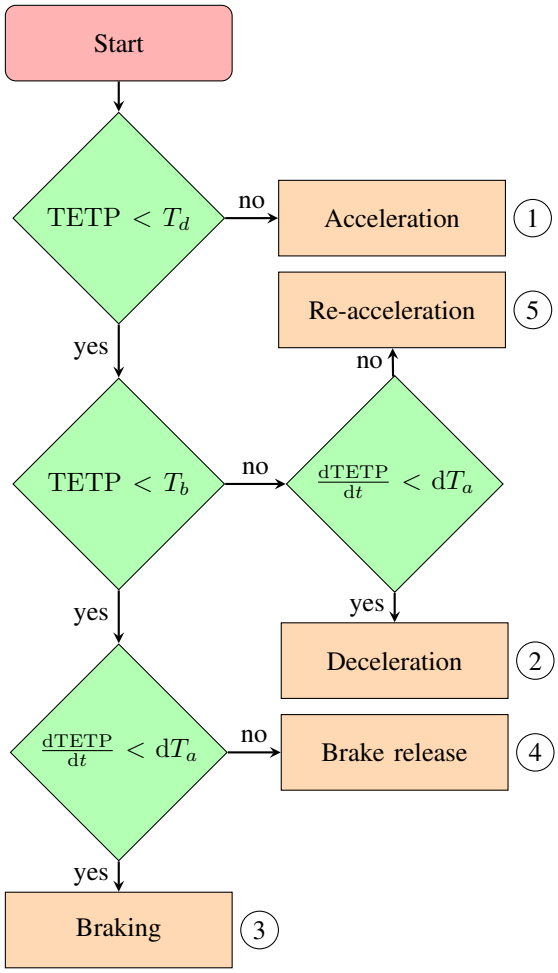

Fig. 3. Model phase decision flowchart

$$\delta_a = \min\left(\delta_{a,EB} + K_a\left(1 - \frac{V}{V_{max}}\right), K_a\left(\frac{\mathrm{dTETP}}{\mathrm{d}t} - \mathrm{d}T_a\right)\right) \tag{4}$$

5) *Re-acceleration*: This phase is entered when the TETP is between T_b and T_d, but its rate of change is above $\mathrm{d}T_a$. In this case, the driver feels safe enough to begin accelerating again. The brake pedal deflection is $\delta_b = 0$, while the accelerator pedal is the minimum value between the one found for the acceleration phase, and the value derived from Eq. 5. This calculation is similar to the one in the deceleration phase, but uses the acceleration gain K_a instead of K_d.

$$\delta_a = \min\left(\delta_{a,EB} + K_a\left(1 - \frac{V}{V_{max}}\right), K_a\left(\frac{\text{TETP} - T_b}{T_d - T_b}\right)\right) \tag{5}$$

Fig. 4. The fixed-base driving simulator at the Faculty of Aerospace Engineering of the Delft University of Technology.

III. Experiment

An experiment was set up at the fixed-base driving simulator in the HMI Laboratory, at the Faculty of Aerospace Engineering of TU Delft, in order to satisfy three goals:

1) Show that the proposed TETP-based speed model can capture general trends of driver speed adaptation to a range of road geometry (road width, corner radii and deflection angles).
2) Provide evidence for the phases of speed adaptation, and show that TETP triggers can explain these phases more accurately than TLC (an alternative time-based metric).
3) Provide validation data in order to individualize the model, and measure its performance in reproducing individual drivers' speed control strategies.

A. Apparatus

In the fixed-base driving simulator, Figure 4, an LCD screen was used to show speedometer information, while three projectors displayed the driving scene, generating a field of view over 180 degrees. Engine sound was played through speakers to aid in speed perception. The simulated vehicle was a heavy sedan equipped with an automatic 4-speed gearbox.

B. Design

The experiment was performed by sixteen participants (3 female, 13 male), with mixed experience (age 25 ± 2 years, licensed since 6.1 ± 2.6 years, driving 4600 ± 4200km per year). Data from one participant were incomplete due to motion sickness.

Six different roads were used, with alternating turns and straight sections, with two road widths (3.6m and 2.4m), and two corner radii for the turns (150m and 300m), and two deflection angles (45 and 90 degrees), an example is given in Figure 5. In order to improve visual speed perception, the road was lined with poles spaced at regular intervals, and trees were placed in the scenery.

Subjects were instructed to drive as they would in a real world driving situation, adapting their speed and steering behavior in order to stay within the lane boundaries. They were told the roads allowed only for one-way traffic, and that they could use all of the available road width. They were requested to treat the speed limit of 100kmh^{-1} in the same manner they would treat a speed limit on a real road.

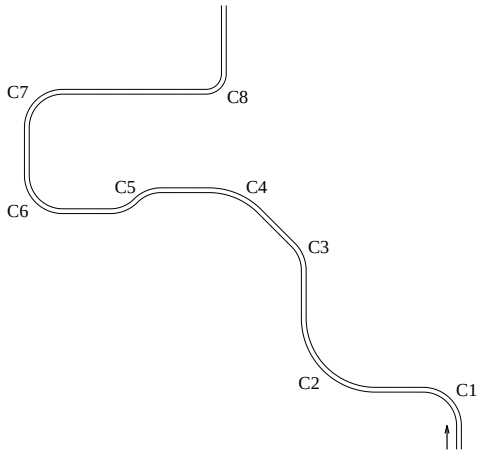

Fig. 5. Road 3 of the experiment (road width not to scale).

IV. Experimental Results and Model fit

Using the driving experiment data, the relevant parameters for the speed control model were calculated and plotted for inspection. Figure 6 shows a typical result. The pedal trace shows the distinct phases. As the car approaches the curve, the TETP decreases linearly. The driver releases the gas pedal once a certain TETP threshold, indicated by the dashed vertical line, has been passed, at approximately 50m before the corner. After releasing the gas pedal, the TETP continues to decrease, eventually causing the driver to apply the brakes (solid vertical line). Once the TETP stops decreasing, the driver feels comfortable enough to begin re-accelerating, and after the TETP has increased past any thresholds, the driver eventually increases the acceleration.

The figure shows the value of using TETP triggers for modeling speed adaptation: at a TETP of approximately $3s$ the driver releases the gas pedal, followed by braking at a TETP of approximately $2.3s$. Comparison to the TLC, shown in the same figure, show that TETP is a better candidate for curve speed modeling applications.

A. Individual driver parameter fit

Two-thirds of the data were used to fit the TETP thresholds for decelerating and for braking, T_d and T_b respectively. We used the Matthews Correlation Coefficient (MCC) as a measure for the classifier [20], since this has been shown to perform well even when the sizes of the two classifications are very different [21], as was the case for our data. A confusion matrix was set up (as in Table I), and the classifier:

$$MCC = \frac{n_{TP} \cdot n_{TN} - n_{FP} \cdot n_{FN}}{\sqrt{(n_{TP} + n_{FP})(n_{TP} + n_{FN})(n_{TN} + n_{FP})(n_{TN} + n_{FN})}} \quad (6)$$

was evaluated. T_d and T_b were varied to find the maximum classifier values. The remaining parameters were found by a

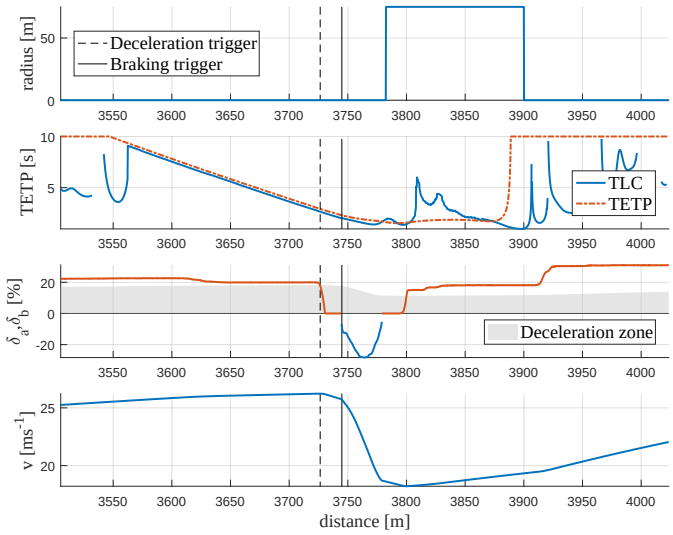

Fig. 6. Typical example (S15) of the variation of TETP, TLC, speed, and pedal deflections on a 75m radius right turn. Positive pedal deflections correspond to the accelerator pedal, while negative deflections represent brake actuation. The shaded area represents the deceleration zone, that is, the accelerator pedal position values that correspond to a zero or negative acceleration.

constrained least squares fit between the combined accelerator and brake pedal trace of the model and recorded data. $\mathrm{d}T_a$ was allowed to vary from -0.5 to 0, K_a, K_d and K_b from 0.01 to 10. Since differences in speed behavior between subjects was expected, and also observed later in the data, the model fit was performed for each subject individually. The group average and standard deviation of the parameter values are given in Table II.

TABLE I
CONFUSION MATRIX FOR ACCELERATOR PEDAL RELEASE

	$\mathrm{TETP} \leq T_d$	$\mathrm{TETP} > T_d$
$\delta_a \leq \tilde{\delta}_{a,EB}$	TP	FN
$\delta_a > \tilde{\delta}_{a,EB}$	FP	TN

B. Validation

One third of the data was reserved for validation. In literature, speed control models are usually judged on their performance in a single turn [2], [4], [7]. In this case, the model was initialized on a straight segment approximately 500m before a 75m radius 90 degree turn. The global results of this validation are given in Figure 7, while Figure 8 shows an example of the model performance. Variance Accounted For (VAF) for the speed (V) shows fair results, predicting

TABLE II
AVERAGE IDENTIFIED PARAMETERS FOR ALL SUBJECT, AND SET OF PARAMETERS FOR THE INITIAL MODEL SIMULATION

	T_d [s]	T_b [s]	K_d [-]	K_b-	K_a [-]	$\mathrm{d}T_a$ [-]
Mean	4.6673	3.2597	0.6504	4.1488	0.9801	-0.2259
StdDev	1.4342	1.1286	0.7130	1.4776	0.0460	0.0657
Simulation	3.8	2.8	1	5	1	-0.25

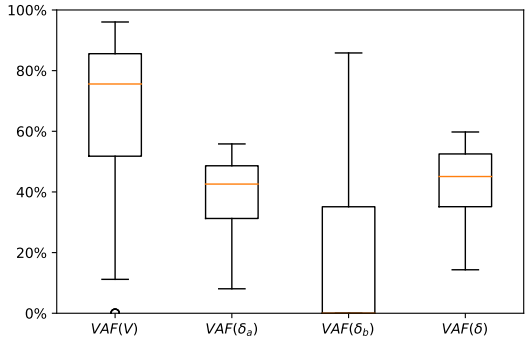

Fig. 7. Evaluation of the TETP speed control model performance for a wide and a narrow isolated turn with 75m radius.

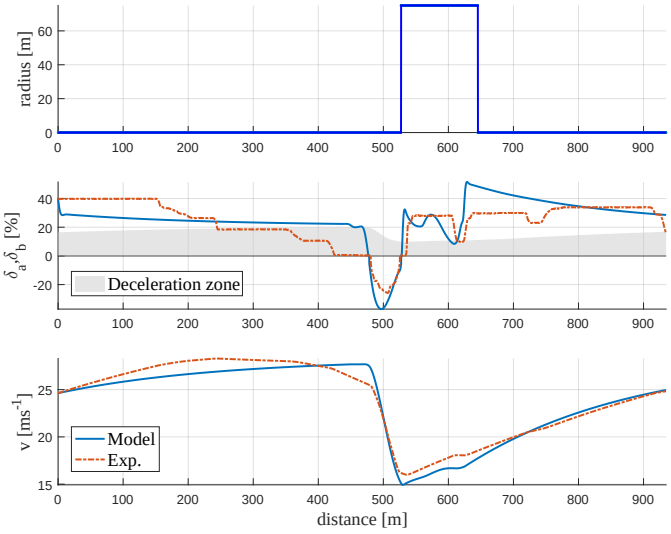

Fig. 8. Example (S4) of the performance of the model on an isolated 75m radius turn. Positive pedal deflections correspond to the accelerator pedal, while negative deflections represent brake actuation. The shaded area represents the deceleration zone, that is, the accelerator pedal position values that correspond to a zero or negative acceleration.

the accelerator pedal trace (δ_a) and in particular brake timing works well for only a part of the participants. Combined acceleration/brake pedal prediction ($(VAR(\delta))$) is fair. In the example, the model accurately tracks the speed and pedal deflections, the only significant mismatch is the fact that the real driver releases the gas pedal slightly earlier than the model and coasts for approximately 50m before applying the brakes. The braking event timing is also accurate, with a small difference in magnitude of brake pedal actuation caused by the difference in speed at the onset of braking due to the extra coasting. The short release of the accelerator pedal on curve exit is also reproduced.

Validation results showed that, for most subjects, the TETP-based model can accurately track driver speed choice in an isolated turn, with an average speed VAF above 60%. The acceleration and gas pedal deflection VAF values are lower,

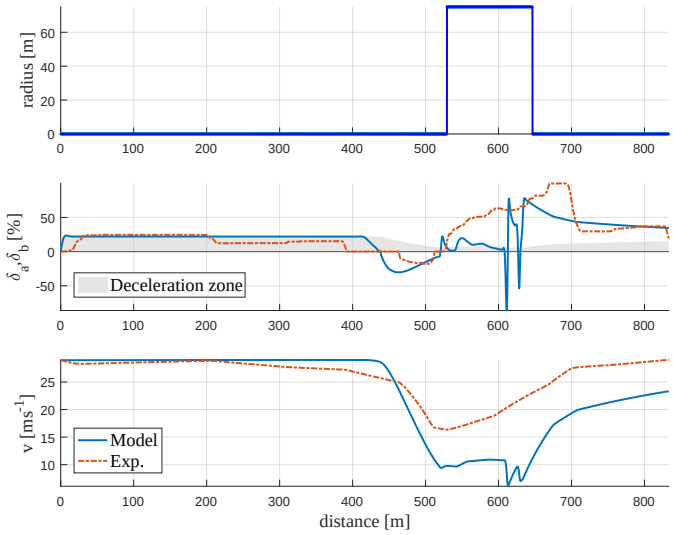

Fig. 9. An example of decreased model performance, subject 6, narrow road.

but the fact that they are, on average, above 30% can be seen as a corroboration for the speed results. The brake pedal deflection VAF values are low, but this can be attributed to the fact that there are only few occasions where drivers actually use the brake pedal, resulting in low variance overall. VAF results show large variability, with a standard deviation of the speed VAF of approximately 30%. For four of the subject/road combinations the speed VAF is below 25%. An example of poorly fitted data is shown in Figure 9, indicating that modeling the relationship between TETP and pedal actuation must still be improved. Some subjects use larger values of T_d, for different reasons. Subject 6 drove at consistently high speeds ($v_{avg} = 26.8\text{ms}^{-1}$), released the accelerator pedal relatively early and braked as little as possible, while Subject 9 drove at comparatively low speeds ($v_{avg} = 20.1\text{ms}^{-1}$) throughout the experiment and started the brake phase early, as evidenced by a T_b value of 6.29s.

V. Conclusions

Unlike many existing models, this research directly relates visual perception to pedal control when driving on a curved road. The two thresholds on a single perceptual variable, the Time to Extended Tangent Point, allow for a model that distinguishes acceleration, coasting and braking phases. By modeling individual driver's speed adaptation including pedal control behaviour, we enable future research towards individualized ADAS and self-driving vehicles. More specifically, this research paves the way for haptic shared control systems that integrate longitudinal [13], [22] and lateral support [23], potentially allowing drivers to feel the tightness of upcoming turns through forces on the gas pedal.

References

[1] P. Bosetti, M. Da Lio, and A. Saroldi, "On the human control of vehicles: an experimental study of acceleration," *European Transport Research Review*, vol. 6, no. 2, pp. 157–170, 2013.

[2] M. Shino, H. Yoshitake, M. Hiramatsu, T. Sunda, and M. Kamata, "Deviated state detection method in driving around curves based on naturalistic driving behavior database for driver assistance systems," *International Journal of Automotive Technology*, vol. 15, no. 5, pp. 749–755, Aug. 2014.

[3] S. Cafiso and G. Cerni, "A new approach to define continuous Speed Profile Models for two lane rural roads," en, *Transportation Research Record*, vol. 23-09, no. July, pp. 1–22, Dec. 2012.

[4] A. M. C. Odhams and D. J. Cole, "Models of driver speed choice in curves," in *7th International Symposium on Advanced Vehicle Control (AVEC 04)*, 2004.

[5] A. Montella, L. Pariota, F. Galante, L. L. Imbriani, and F. Mauriello, "Prediction of Drivers ' Speed Behaviour on Rural Motorways Based on an Instrumented Vehicle Study," *Transportation Research Record: Journal of the Transportation Research Board*, no. 2434, pp. 52–62, 2014.

[6] B. Turner, J. Woolley, and P. Cairney, "An analysis of driver behaviour through rural curves: Exploratory results on driver speed," in *Australasian Road Safety Conference*, 2015.

[7] D. Zhang, Q. Xiao, J. Wang, and K. Li, "Driver curve speed model and its application to ACC speed control in curved roads," *International Journal of Automotive Technology*, vol. 14, no. 2, pp. 241–247, Mar. 2013.

[8] W. H. Levison, A. Bittner, J. Campbell, and C. Schreiner, "Modification and Partial Validation of the Driver/Vehicle Module," en, *Transportation Research Record: Journal of the Transportation Research Board*, vol. 1803, pp. 52–58, Jan. 2002.

[9] Y. Shao, J. Xu, B. Li, and K. Yang, "Modeling the Speed Choice Behaviors of Drivers on Mountainous Roads with Complicated Shapes," *Advances in Mechanical Engineering*, vol. 7, no. 2, pp. 862 610–862 610, Feb. 2015.

[10] B. N. Fildes and T. J. Triggs, "The Effect of Road Curve Geometry on Curvature Matching Judgements," *Australian Road Research*, vol. 12, no. 5, p. 63–70, 1984.

[11] H. Summala, "Risk control is not risk adjustment: the zero-risk theory of driver behaviour and its implications," *Ergonomics*, vol. 31, no. 4, pp. 491–506, 1988.

[12] H. Godthelp and W. van Winsum, "Speed Choice and Steering Behavior in Curve Driving," *Human Factors: The Journal of the Human Factors and Ergonomics Society*, vol. 38, no. 3, pp. 434–441, 1996.

[13] D. A. Abbink, E. R. Boer, and M. Mulder, "Motivation for continuous haptic gas pedal feedback to support car following," *IEEE Intelligent Vehicles Symposium, Proceedings*, pp. 283–290, 2008.

[14] E. R. Boer, "Car following from the driver's perspective," *Transportation Research Part F: Traffic Psychology and Behaviour*, vol. 2, no. 1999, pp. 201–206, 2000.

[15] M. F. Land and D. N. Lee, "Where we look when we steer," *Nature*, vol. 369, no. 6483, pp. 742–744, 1994.

[16] E. R. Boer, "Tangent point oriented curve negotiation," in *Proceedings of the 1996 IEEE Intelligent Vehicles Symposium*, Tokyo: IEEE, 1996, pp. 7–12.

[17] E. Lehtonen, O. Lappi, and H. Summala, "Anticipatory eye movements when approaching a curve on a rural road depend on working memory load," *Transportation Research Part F: Traffic Psychology and Behaviour*, vol. 15, no. 3, pp. 369–377, 2012.

[18] O. Lappi, P. Rinkkalla, and J. Pekkanen, "Systematic Observation of An Expert Driver's Gaze Strategy - An On-Road Case Study," *Frontiers in Psychology*, vol. 8, no. April, 2017.

[19] T. Melman, J. C. de Winter, and D. A. Abbink, "Does haptic steering guidance instigate speeding? A driving simulator study into causes and remedies," *Accident Analysis and Prevention*, vol. 98, pp. 372–387, 2017.

[20] B. W. Matthews, "Comparison of the predicted and observed secondary structure of T4 phage lysozyme," *Biochimica et Biophysica Acta (BBA)-Protein Structure*, vol. 405, no. 2, pp. 442–451, 1975.

[21] D. M. W. Powers, "Evaluation: From Precision, Recall and F-Factor to ROC, Informedness, Markedness & Correlation David," *Journal of Machine Learning Technologies*, vol. 2, no. December, pp. 37–63, 2007.

[22] M. Mulder, M. Mulder, M. M. van Paassen, and D. A. Abbink, "Haptic gas pedal feedback," *Ergonomics*, vol. 51, no. 11, pp. 1710–1720, 2008.

[23] D. A. Abbink, M. Mulder, and E. R. Boer, "Haptic shared control: Smoothly shifting control authority?" *Cognition, Technology and Work*, vol. 14, pp. 19–28, 2012.